

Fluorescence axial nanotomography with plasmonics

Nicholas I. Cade,^{ab} Gilbert O. Fruhwirth,^{cd} Alexey V. Krasavin,^a Tony Ng^c and David Richards^{*a}

Received 7th October 2014, Accepted 16th October 2014

DOI: 10.1039/c4fd00198b

We present a novel imaging technique with super-resolution axial sensitivity, exploiting the changes in fluorescence lifetime above a plasmonic substrate. Using conventional confocal fluorescence lifetime imaging, we show that it is possible to deliver down to 6 nm axial position sensitivity of fluorophores in whole biological cell imaging. We employ this technique to map the topography of the cellular membrane, and demonstrate its application in an investigation of receptor-mediated endocytosis in carcinoma cells.

1 Introduction

Plasmonic nanostructures have received considerable attention in recent years for their promise as new sensing platforms. This attention has focused principally on the strong confinement of electromagnetic fields, leading to exquisite sensitivity of localised surface plasmon resonances (LSPRs) to the local refractive index and to surface enhanced Raman spectroscopy, both approaches providing high sensitivity to surface-bound molecules. Here we illustrate the power of thin film plasmonics to additionally provide high sensitivity to variations in the spatial distribution of fluorescent molecules within a hundred nanometres of a metal surface, by exploiting modifications to the radiative and non-radiative decays experienced by the molecules.

A range of fluorescence imaging techniques have emerged in recent years which are able to provide spatial super-resolution in three dimensions,^{1,2} enabling the nanoscale mapping of cellular structures. However, generally these techniques do not retain compatibility with live cell imaging, while there are inevitable compromises on imaging speed and area. On the other hand, in many

^aDepartment of Physics, King's College London, Strand, London WC2R 2LS, UK. E-mail: david.r.richards@kcl.ac.uk; Fax: +44 (0)20 7848 2420; Tel: +44 (0)20 7848 2753

^bCancer Research UK, London Research Institute, 44 Lincoln's Inn Fields, London WC2A 3LY, UK

^cRichard Dumbleby Department of Cancer Research, Division of Cancer Studies, Randall Division of Cell & Molecular Biophysics, King's College London, London SE1 1UL, UK

^dDepartment of Imaging Chemistry & Biology, Division of Imaging Sciences & Biomedical Engineering, King's College London, London SE1 7EH, UK

cases the lateral resolution of >200 nm achievable with conventional confocal or multiphoton microscopy is in fact sufficient, and it is the diffraction-limited resolution of >500 nm along the optical axis (perpendicular to the substrate surface) which limit their effectiveness for the measurement of subtle spatial dynamics of molecules, such as receptors in a cell membrane. Although wide-field microscopies such as total internal reflection (TIRF) microscopy^{3,4} and fluorescence interference contrast microscopy (FLIC)⁵ do enable axial resolution <100 nm, the encoding of the axial position of fluorophores through fluorescence intensity is hindered by photo-bleaching and variations in labelling homogeneity, while these techniques are also only sensitive to fluorophores very close to the substrate surface.

We have previously demonstrated that confocal fluorescence lifetime imaging (FLIM) of cells adhered on both smooth⁶ and nanostructured⁷ noble metal films can be used to precisely determine the axial position of fluorescent molecules up to about 100 nm above the surface, with an axial position sensitivity of less than 10 nm in whole cell imaging, offering significant advantages over other methods for monitoring the redistribution of fluorophores above a surface. In particular, changes in fluorescence lifetime are insensitive to changes in fluorescence intensity, either from variations in expression levels or from photo-bleaching. We have demonstrated that this technique provides a novel bioassay for screening cell receptor internalisation,^{6,7} enabling the sensitive measurement of the redistribution of proteins in a cell during endocytosis, even when averaging over a large area. For membrane-bound fluorophores, the measured lifetime variation can be converted into an absolute distance above the substrate for tomographic imaging with super-resolution accuracy, thereby providing information on changes in membrane morphology during dynamic processes.⁷

Cell imaging performed using a flat gold film,⁶ which has also been demonstrated subsequently by Chizhik *et al.*,⁸ exploits the large increase in non-radiative damping, and hence the reduction in the fluorescence lifetime, of molecules located at sub-wavelength separations above a smooth gold film.^{9–11} However, in this approach, there is either a loss of signal from imaging through a semi-transparent film, or it is necessary to image through the sample from above. The latter case increases the background fluorescence in thick samples and limits the collection numerical aperture; furthermore, this geometry is not suitable for studying live biological processes when normally the sample would be excited from below using an inverted microscope.

Efficient excitation through the film is made possible with the use of a large area nanostructured plasmonic thin film.⁷ This maintains the flexibility and lateral resolution of a standard confocal configuration suitable for use in live-cell imaging; in addition, the nanostructured film can be designed to optimise the spectral overlap of the localised surface plasmon resonances of the metal nanostructure with the molecular fluorescence, to achieve the greatest lifetime sensitivity and signal enhancement. In this case, the Purcell effect also leads to an enhancement in radiative decay,¹² resulting in an increase in fluorescence intensity alongside a reduction in fluorescence lifetime, for molecules in close proximity to the nanostructure surface.¹³

We report here on the application of nanostructured plasmonic thin films, in combination with fluorescence lifetime imaging, for axial nanotomography of

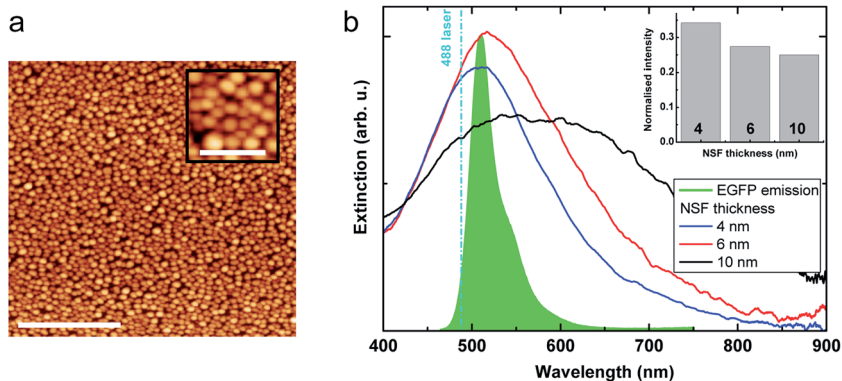


Fig. 1 (a) AFM image of a silver film with a 6 nm nominal Ag thickness; scale bar is 2 μm . Inset: enlarged region; scale bar is 500 nm. (b) Extinction spectra for large area nanostructured silver films (NSFs) of nominal thickness 4 nm (blue line), 6 nm (red) and 10 nm (black). Also shown is the emission spectrum of eGFP (filled green), and the 488 nm excitation laser. Inset: fluorescence intensity from cells on a NSF normalised to those on a nearby area of glass (a scratch in the silver film) for NSFs of different nominal thickness.

cells; in particular, we compare directly their use with that of flat solid metal films.

2 Experimental methods

2.1 Plasmonic substrates for cell culture and imaging

We have developed nanostructured silver films, comprising densely-packed self-organised distributions of silver nanoparticles, that can be easily and inexpensively manufactured over large continuous areas by thermal vacuum deposition.^{7,14} A 1.3 nm layer of Cr was first thermally evaporated onto 0.2 mm glass coverslips (Agar Scientific, UK) to increase the adherence of Ag, followed by Ag with a nominal thickness of between 4 and 10 nm, in a vacuum chamber at 10^{-6} Torr (U300, Oerlikon Leybold, Germany). The evaporation rate (0.05 nm s^{-1}) and nominal metal thickness were measured during evaporation with a quartz crystal oscillator (E5550; Quorum Technologies, UK). The films were subsequently annealed for 30 min at 190 $^{\circ}\text{C}$ in an Ar atmosphere to create a nanostructured surface with a strong plasmon resonance; the nominal deposited thickness of the silver film and subsequent annealing allows the peak of the LSPR spectrum to be tuned to the required value.¹⁵ Atomic force microscopy (AFM) images (see *e.g.* Fig. 1a) acquired in tapping mode (Caliber, Veeco Instruments, CA) and analyzed using Gwyddion 2.21 (<http://gwyddion.net>), indicate that the films consist of individual semi-spheroidal nanoparticles, closely packed with a density and diameter dependent on the nominal evaporated thickness of the film. The extinction spectra from the nanostructured silver films with different nominal thicknesses are shown in Fig. 1b, indicating a strong LSPR of these nanostructures, providing good spectral overlap with the emission spectrum of enhanced green fluorescence protein (eGFP).

For compatibility with cell culture, nanostructured silver films were coated with *N*-(2-mercaptopropionyl)glycine (MPG) which forms a protective monolayer

over the silver and significantly lowers its cytotoxicity.¹⁶ Coated coverslips were immersed in a 1 mM solution of MPG for 60 min at room temperature. Subsequently, the coverslips were twice washed with phosphate buffered saline (PBS, pH = 7.4) and sterilized by submerging into 70% (v/v) ethanol for 60 min. Before the seeding of cells, the coverslips were thoroughly washed with PBS to remove any traces of ethanol.

Flat gold surfaces were prepared by deposition of 30 nm-thick gold films on sixteen-well LabTek chamber slides (Thermo Fisher Scientific, Denmark) by thermal evaporation of gold (as above). The slides were disassembled before evaporation, and then reassembled and tested for integrity. No further treatment was required for cell culture.

2.2 Cell culture and treatment

The DNA of the human chemokine receptor CXCR4 was fused to the N-terminus of enhanced green fluorescent protein (GFP) and the resulting plasmid was used to generate a mammary adenocarcinoma cell line stably expressing CXCR4-GFP, as described elsewhere.¹⁷ Cells were trypsinised for 5 min, seeded onto the metal-coated slides, and grown to the desired cell density. The cells exhibited normal growth on both MPG-treated nanostructured silver films and gold films, with the MPG coating preventing silver-induced cytotoxicity. Subsequently, cells were fixed in 4% (w/v) paraformaldehyde for 15 min, washed with PBS and rinsed with deionized water, before the samples were mounted in Mowiol 488 containing 2.5% (w/v) Dabco. All standard chemicals were either from Sigma-Aldrich (UK) or VWR (UK).

2.3 Fluorescence lifetime imaging

Fluorescence lifetime and intensity images of nanostructured silver film coated slides were obtained by imaging through the coverslip and silver film in a conventional inverted microscope geometry. A confocal microscope (TE2000E, Nikon Corporation, Japan) with custom built scanning stage was used with a 100× oil immersion lens (1.45 NA; Leica, Germany). Photon detection was carried out with an avalanche photodiode (Id-100; Id Quantique, Switzerland) and a synchronous time-correlated single photon counting (TCSPC) module (SPC-150; Becker & Hickl, Germany), with a band-pass filter (550/88, Semrock, IL) fitted before the detector. Excitation was at 488 nm and 20 MHz using a super-continuum laser (SC-450-2; Fianium, UK), with the output sent through a monochromator, laser line filter (488IN, Comar, UK), and beam expander.

Measurements of Au-coated slides were performed using a scanning confocal microscope (TCSP2; Leica, Germany) scanning at 400 Hz with a 63× oil immersion lens (1.4 NA; Leica), through a coverslip placed over the sample. Photon detection was with a photomultiplier tube (PCM-100; Becker & Hickl, Germany) and a synchronous TCSPC module (SPC-830; Becker & Hickl). A 464 nm long-pass filter (XE458; Omega Optical, USA) and EGFP band-pass filter (525/50M; Chroma Technology, USA) were fitted before the detector. Excitation was at 442 nm and 76 MHz using a Ti:Sapphire laser (Mira 900; Coherent Laser, USA) with frequency doubler.

All measurements were acquired in the focal plane of the metal surface, except where indicated. The laser power was adjusted to give average photon counting

rates below the maximum rate of the photon counting electronics and far below the fluorescence saturation level. The photon arrival times were binned into 256 time windows over a period of 10–25 ns. Spatially resolved FLIM images of cells were acquired for 300–600 s at a resolution of 256×256 pixels. The data was typically binned with a radius of 2–5 pixels, and the decay transient for each pixel bin was fitted with a mono-exponential fit after correcting for background fluorescence and an instrument response time of ~ 180 ps (SPCImage, Becker & Hickl). The intensity of the resulting lifetime image was weighted with the total fluorescence intensity at each point.

3 Distance calibration

Fluorescent molecules in close proximity to a gold or silver surface (smooth or nanostructured) experience a modification of their fluorescence lifetime which is dependent on their separation from the surface. This provides a means for the determination of the axial position of a fluorophore from a noble metal surface, as we and others have shown,^{7,8,18} provided there exists a calibration of the dependence of the modified fluorescence lifetime with the separation.

We have obtained an empirical calibration of the axial position using microbeads surface labeled with fluorescein isothiocyanate (FITC) (M0162; Sigma, Gillingham, UK) (such that they closely mimic the geometry of membrane labelled cells, with photophysical properties similar to eGFP). The spherical geometry of the beads, of known diameter $2R$ (6–10 μm), permits the determination of the separation d of fluorophores from the plane of contact, using the radial distance r from the centre of symmetry (identified with the point of contact) in the FLIM images (see Fig. 2a).^{6,7}

200 μL of the microspheres were centrifuged at 5000 rpm for 2 min, the supernatant was removed, 100 μL of Mowiol (ICN, USA) containing Dabco as an antifade was added and well mixed, and a few drops of the microspheres were placed on a slide and covered with a glass coverslip. Fluorescence lifetime images of the microbeads were then acquired in the plane of the metal film surface (flat gold or nanostructured silver film), imaging only close to the point of contact, where the bead surface is close to the substrate surface and the surface-labelled fluorophores lie within the excitation focal volume. The lateral resolution of ~ 250 nm in our diffraction-limited confocal images means that our measurements average over a small range of axial separations. In the case of the nanostructured silver film substrate, this also results in FLIM measurements averaging typically over a number of silver nanoparticles at any given point (see Fig. 1a), such that it can be considered to be effectively a smooth surface.

For both types of surface, a reduction in the fluorescence lifetime is observed around the centre of the microsphere image, corresponding to locations where the fluorophores bound to the microsphere surface are close to the metal surface. For the flat gold film, there was an associated reduction in fluorescence intensity while, for the nanostructured silver film substrate, we observed a two-fold increase in fluorescence intensity, commensurate with the decrease in fluorescence lifetime. Lifetime analysis was performed with a constant bin radius of 3 pixels (~ 250 nm), and the fluorescence lifetime image was then radially averaged around the point of contact (constant r), to obtain a distance–lifetime profile. The average profiles for both nanostructured silver and flat gold film substrates are

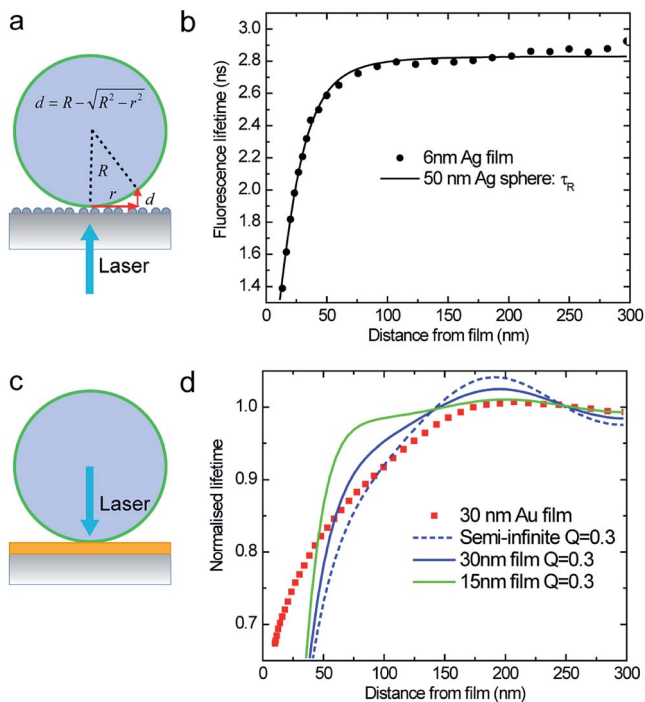


Fig. 2 Distance-dependence characterisation of fluorescence modification by a nanostructured silver film of nominal thickness 6 nm (a and b) and a flat 30 nm-thick gold film (c and d), using fluorescence lifetime imaging (FLIM) of FITC-surface-labelled micro-beads deposited on the surfaces. (a and c) Schematic illustrations of the measurements, indicating in (a) the method of determination of the fluorophore-surface separation, d , from the distance from the centre of the micro-bead FLIM image, and the known radius, R , of the micro-bead. (b and d) Fluorescence lifetime, normalised to the unmodified eGFP lifetime as a function of the axial distance above the surface. (b) For the nanostructured silver film, obtained by radially averaging the images from 3 beads of different diameter; the solid line is the polarization-averaged radiative lifetime τ_R of a dipole as a function of the distance away from a 50 nm Ag sphere in water, calculated at an emission wavelength of 510 nm. (d) Fluorescence lifetime dependence for the flat gold film obtained by radially averaging the FLIM image of an 8 μm diameter micro-bead. The continuous lines show the polarization-averaged radiative lifetime of a dipole, in water, as a function of the distance away from a Au film of thickness 15 nm (solid green line), 30 nm (solid blue line) and semi-infinite (dashed line), calculated at an emission wavelength of 510 nm and an unmodified quantum yield of 0.3.

shown in Fig. 2, with a rapid reduction in both cases in the fluorophore lifetime as the separation from the metal surface decreases. However, while the flat gold film indicates already a high degree of distance sensitivity of ~ 20 nm per 100 ps for separations less than 50 nm, the nanostructured silver film provides a much higher sensitivity of ~ 3 nm per 100 ps within ~ 50 nm of the surface.

The results of a theoretical analysis of the expected dependence of fluorescence lifetime on separation from the metal film are also shown in Fig. 2. The nanostructured silver film was modelled as an approximately homogeneous array of uncoupled spherical silver spheres in water, with the fluorescence lifetime of a FITC molecule calculated using a dipole-dipole model, as a function of the

separation from the sphere;^{19,20} the nanoparticle radius was taken to be 50 nm, corresponding to the average radius and height of the nanoparticles measured with AFM for the nanostructured silver film (of nominal thickness 6 nm). Decay rates were averaged over the tangential and radial orientations of the emitting dipole assuming an isotropic distribution, for an emission wavelength of 510 nm, with an excellent agreement with the experimental data (Fig. 2b); these calculations indicate that the reduction in the fluorescence lifetime is dominated by an enhancement in radiative decay. We note that the diffraction limited measurement, over a number of nanoparticles and a large number of molecules around the point of contact of the micro-bead, results in insensitivity to separations less than ~ 10 nm, such that our measurements do not probe the expected reduction of emission intensity at very small separations.^{21,22}

On the other hand, in the case of a flat gold film (Fig. 2d), for separations less than 50 nm, the observed behaviour could not be reproduced from calculations of the expected fluorescence lifetime dependence (averaged over the tangential and radial orientations of the emitting dipole),^{23,24} with the experiment demonstrating a slower change in lifetime than that predicted theoretically. Unlike a nanostructured film, for which an enhancement in fluorescence intensity and radiative decay rate occurs with the decreasing separation, fluorescence is quenched as a fluorophore approaches a flat gold surface, associated with an increase in only the non-radiative decay rate, from the non-radiative energy transfer to surface plasmons and the direct power dissipation in the gold film. The consequence of this is that, given the limited axial and lateral resolution of confocal imaging, few photons are detected from the molecules closest to the gold film: the fluorescence lifetime decay determined using TCSPC originates from fluorescence further away from the surface (although within the focal area), while the low signal levels also result in greater errors in the lifetime determination. The net effect of this is that, in reality, the first part of the empirical curve corresponds to larger distances, accounting for the departure from the theoretical prediction for separations less than 50 nm. The calculated fluorescence lifetime dependence for a flat gold film is also strongly dependent on both the fluorophore quantum yield and the thickness of the gold film, with a quantum yield of only 0.3 providing the best agreement for large separations.

The measured dependence of the fluorescence lifetime on the fluorophore separation from the metal film surface provides an empirical calibration of the separation as a function of the fluorescence lifetime in FLIM. There are, however, various sources of measurement error which limit the axial sensitivity of this approach. Firstly, the sensitivity to lifetime variations is limited by the instrumental response of the system of 180 ps, which is convolved with the fluorescence decay. Low photon counts can also limit significantly mono-exponential fits of the fluorescence decay and, as identified above, these can be dominant in the case of small separations in flat gold films. For nanostructured silver films, the accuracy in the relative sample height above the film is limited by the distribution in the nanoparticle heights within a binned area of the FLIM image (approximately the size of the confocal spot, ~ 250 nm); from the AFM height analysis, this is approximately ± 5 nm. Propagating these uncertainties, we estimate for nanostructured silver substrates an error in the final height map of approximately ± 6 nm when closest to the film and ± 12 nm for distances ~ 65 nm.

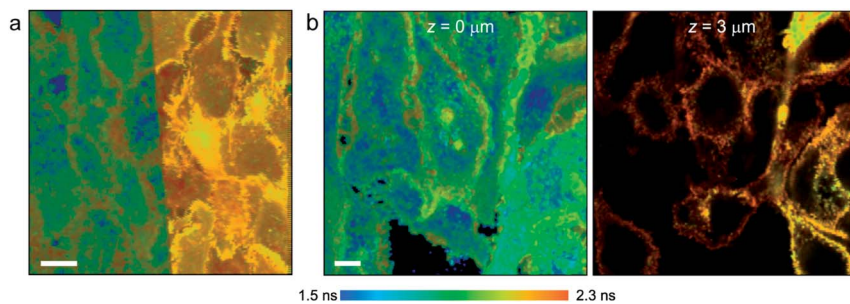


Fig. 3 Fluorescence lifetime images (intensity weighted) of carcinoma cells expressing eGFP on the CXCR4 membrane receptor: (a) at a NSF (left)–glass (right) boundary; scale bar 10 μm ; (b) from a region of cells on a NSF, when imaging in the plane of the nanostructured silver film (left) and 3 μm above the NSF (right); scale bar 5 μm .

4 Nanotomography of biological cells

Metal-coated glass coverslips were then employed in a fluorescence imaging study of mammary carcinoma cells expressing the chemokine receptor CXCR4 C-terminally fused to eGFP at the plasma membrane (so eGFP is at the cytosolic side of the membrane). Fig. 3a shows a FLIM image of cells at the boundary between uncoated glass and a nanostructured silver film with a nominal film thickness of 6 nm. On the glass region, the cells have a very narrow lifetime distribution around that expected for eGFP; in contrast, similar cells on the nanostructured silver film show significant lifetime reduction, indicating that the eGFP is located within 50 nm of the surface. FLIM images acquired from a focal plane a few microns above the nanostructured silver film show no reduction in lifetime, compared to those acquired in the plane of the film (Fig. 3b), confirming that the lifetime modification occurs only over a small distance above the silver nanostructure. Note that such measurements >100 nm from the substrate would not be possible with TIRF.

FLIM of cells cultured on nanostructured silver-coated slides with different nominal film thicknesses, and hence nanoparticle sizes and LSPR extinction spectra (Fig. 1b),¹⁴ all demonstrated the same behaviour. However, the fluorescence intensity was found to be greatest for a nominal thickness of 4 nm, and lower for nominal thicknesses of 6 nm and 10 nm (see inset Fig. 1b). This signal reduction may simply result from the increase in the coating material, although we note that the overlap of the extinction spectrum for the plasmon film with both the excitation wavelength and the eGFP emission is greatest for the 4 nm-film, such that the strongest fluorescence enhancement is expected through resonance with the localised surface plasmons of the silver nanostructure.

High resolution fluorescence intensity and associated fluorescence lifetime images of single cells are presented in Fig. 4, for both nanostructured silver film and flat gold substrates. Small changes in the membrane topography can be identified by the resulting variation in the fluorescence lifetime across the cells and so, height maps were obtained by applying the normalised empirical lifetime calibration (Fig. 2) to the FLIM image data, re-normalised to the unmodified cell fluorescence lifetime (the modal value for cells cultured on glass). We note that

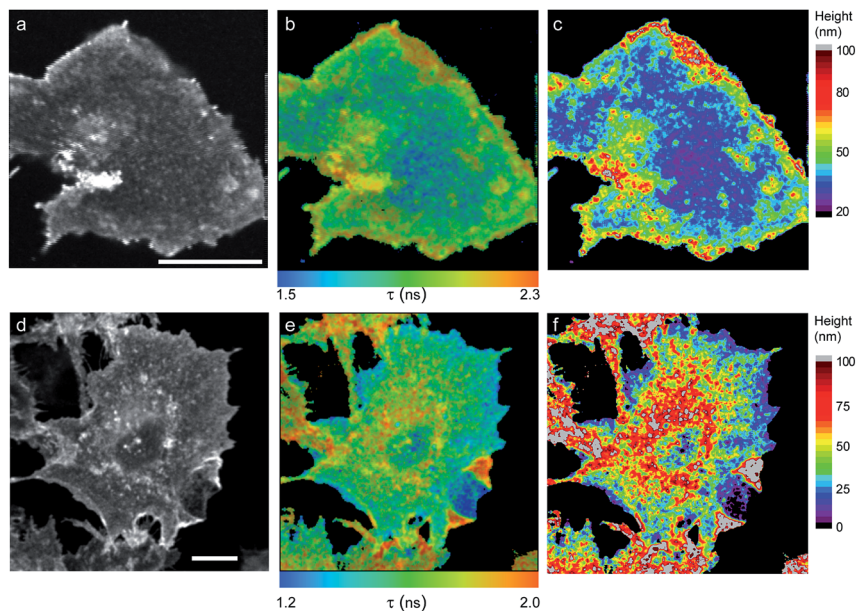


Fig. 4 FLIM and nanotomography of carcinoma cells expressing eGFP on the CXCR4 membrane receptor, cultured on (a–c) a nanostructured silver film (NSF) and (d–f) a flat gold film (scale bars 10 μm). (a and d) Fluorescence intensity and (b and e) fluorescence lifetime, demonstrating the plasmonic assisted reduction in the lifetime of fluorophores expressed in the ventral membrane of the cells. (c and f) Height maps derived from the fluorescence lifetime using calibration curves in Fig. 2; heights were binned in 3 nm intervals. Fluorescence quenching for smaller separations of fluorophores from the flat gold film results in an over-representation of longer lifetimes, such that the height map for the cell cultured on the flat gold film (f) is not considered to be so reliable.

since eGFP is fused to the C-terminus of the CXCR4 receptor, it is separated from the metal films by at least the width of the plasma membrane (~ 10 nm).

For a nanostructured silver film (Fig. 4c), large areas of the basal cell membrane are determined to be 30–50 nm from the substrate, noting that this averages over the diffraction-limited resolution of ~ 250 nm. In addition, the height map also identifies non-attached and vertical parts at the edge of the cell, which have been reported not to be attached to the substrate.²⁵ For the majority of the cell image, the lifetime data is very well fitted by a mono-exponential distribution, which suggests a negligible contribution to the signal from out-of-focus components.

The height map derived for the flat gold substrate (Fig. 4f) presents a very different picture, which we consider does not provide an accurate representation of the height variation of the basal cell membrane. The lower numerical aperture of the objective lens required for imaging from above, due to the opaque substrate, leads to a worse confocal axial resolution, hence resulting in the capture of additional fluorescence from eGFP elsewhere in the cell (*e.g.* other organelles containing CXCR4-eGFP receptors and also the dorsal cell membrane). This is accentuated in the case of a flat gold substrate because the reduction in lifetime is associated with quenching of the fluorescence intensity, such that fluorophores located >100 nm from the substrate with longer fluorescence

lifetimes will provide a greater contribution to the total fluorescence signal. This leads to a distribution of lifetimes, and hence the corresponding height map becomes less reliable in these regions. This is less of an issue with nanostructured substrates, which provide both compatibility with high numerical aperture oil immersion lenses, and also lead to an enhancement (rather than reduction) of the fluorescence intensity for molecules close to the substrate.⁷

5 Conclusions

We have demonstrated that when gold and silver thin films are employed as substrates in biological cell imaging, the distance-dependent modification of the fluorescence lifetime allows the precise determination of the molecular location up to about 100 nm above the substrate surface, providing tomographic imaging of the basal cell membrane with axial super-resolution accuracy.⁷ Changes in the fluorescence lifetime are insensitive to changes in the fluorescence intensity, either from variations in expression levels or from photo-bleaching.

Flat gold films appear at first sight to be attractive for such an application, and we have previously demonstrated the advantages of this approach in a novel FLIM-based assay for screening cell receptor internalisation, in which the fluorescence lifetime provided a very effective yes/no reporter of endocytosis.⁶ However, when using flat metal films, it is the enhancement of non-radiative decay which results in the reduction of the lifetime with the separation from the film; hence, the intensity of the fluorescence signal near the metal is also reduced. This, together with limitations imposed on the collection numerical aperture for opaque substrates, can result in both low signal levels for small separations, making more difficult the reliable determination of the fluorescence lifetime, and in the simultaneous detection of contributions to the fluorescence signal from fluorescent labels both within close proximity of the substrate and also much deeper in the cell, hindering the reliable calibration of the distance from the substrate.

The use of nanostructured plasmonic thin films, on the other hand, provides an axial sensitivity of ~ 6 nm over 100 nm above the nanostructure surface while maintaining the flexibility and lateral resolution of a standard confocal configuration suitable for use in live-cell imaging. For these nanoplasmonic thin films, radiative decay processes dominate, even at close proximity to the metal, leading to higher signal levels from fluorophores close to the substrate. The combination of this and the higher resolution offered by the high numerical aperture lenses available in this case, results in signals derived from well-defined locations within the cell, such as the basal membrane, providing a robust determination of the distance from the substrate from the measured fluorescence lifetime. We have shown elsewhere⁷ that this approach is sensitive to the redistribution of proteins in a cell during endocytosis, even when averaging over a large area, offering significant advantages over other methods.

Acknowledgements

This work was supported by the UK EPSRC (EP/G029806/1). We would also like to acknowledge support from the Cancer Research UK/EPSRC/MRC/DoH-funded KCL and UCL Comprehensive Cancer Imaging Centre C1519/A10331.

References

- 1 X. Zhang, *Nat. Photonics*, 2009, **3**, 365.
- 2 S. W. Hell, R. Schmidt and A. Egnér, *Nat. Photonics*, 2009, **3**, 381.
- 3 A. L. Mattheyses, S. M. Simon and J. Z. Rappoport, Imaging with total internal reflection fluorescence microscopy for the cell biologist, *J. Cell Sci.*, 2010, **123**, 3621–3628.
- 4 D. Axelrod, *Traffic*, 2001, **2**, 764.
- 5 D. Braun and P. Fromherz, *Appl. Phys. A: Mater. Sci. Process.*, 1997, **65**, 341.
- 6 N. I. Cade, G. Fruhwirth, S. J. Archibald, T. Ng and D. Richards, *Biophys. J.*, 2010, **98**, 2752.
- 7 N. I. Cade, G. Fruhwirth, T. Ng and D. Richards, *J. Phys. Chem. Lett.*, 2013, **4**, 3402.
- 8 A. I. Chizhik, J. Rother, I. Gregor, A. Janshoff and J. Enderlein, *Nat. Photonics*, 2014, **8**, 124.
- 9 R. R. Chance, A. H. Miller, A. Prock and R. Silbey, *J. Chem. Phys.*, 1975, **63**, 1589.
- 10 W. L. Barnes, *J. Mod. Opt.*, 1998, **45**, 661.
- 11 E. Fort and S. Grésillon, *J. Phys. D: Appl. Phys.*, 2008, **41**, 013001.
- 12 E. M. Purcell, *Phys. Rev.*, 1946, **69**, 681.
- 13 T. Ritman-Meer, N. I. Cade and D. Richards, *Appl. Phys. Lett.*, 2007, **91**, 123122.
- 14 N. I. Cade, T. Ritman-Meer and D. Richards, *Phys. Rev. B: Condens. Matter Mater. Phys.*, 2009, **79**, 241404.
- 15 K. Aslan, J. R. Lakowicz, H. Szmecinski and C. D. Geddes, *J. Fluoresc.*, 2005, **15**, 37.
- 16 J. Zhang, Y. Fu, D. Liang, R. Y. Zhao and J. R. Lakowicz, *Langmuir*, 2008, **24**, 12452.
- 17 L. S. Vermeer, G. O. Fruhwirth, P. Pandya, T. Ng and A. J. Mason, *J. Proteome Res.*, 2012, **11**, 2996.
- 18 M. Berndt, M. Lorenz, J. Enderlein and S. Diez, *Nano Lett.*, 2010, **10**, 1497.
- 19 R. Carminati, J.-J. Greffet, C. Henkel and J. Vigoureux, *Opt. Commun.*, 2006, **261**, 368.
- 20 A. Moroz, *Opt. Commun.*, 2010, **283**, 2277.
- 21 S. Kühn, U. Håkanson, L. Rogobete and V. Sandoghdar, *Phys. Rev. Lett.*, 2006, **97**, 017402.
- 22 P. Anger, P. Bharadwaj and L. Novotny, *Phys. Rev. Lett.*, 2006, **96**, 113002.
- 23 R. R. Chance, A. Prock and R. Silbey, *J. Chem. Phys.*, 1976, **65**, 2527.
- 24 G. W. Ford and W. H. Weber, *Phys. Rep.*, 1984, **113**, 195.
- 25 J. A. Broussard, W.-H. Lin, D. Majumdar, B. Anderson, B. Eason, C. M. Brown and D. J. Webb, *Mol. Biol. Cell*, 2012, **23**, 1486.